

Frustrated Phase Transformations in Supported, Interdigitating Lipid Bilayers

Babak Sanii,[†] Alan W. Szmodis,[‡] Daniel A. Bricarello,[§] Ann E. Oliver,[§] and Atul N. Parikh^{*,‡,§}

Molecular Foundry, Lawrence Berkeley National Lab, Berkeley, California, Biophysics Graduate Group, University of California, Davis, California, and Department of Applied Science, University of California, Davis, California

Received: September 4, 2009; Revised Manuscript Received: November 16, 2009

In free bilayers, the fluid to gel main phase transition of a monofluorinated phospholipid (F-DPPC) transforms a disordered fluid bilayer into a fully interdigitated monolayer consisting of ordered acyl tails. This transformation results in an increase in molecular area and decrease in bilayer thickness. We show that when confined in patches near a solid surface this reorganization proceeds under constraints of planar topography and total surface area. One consequence of these constraints is to limit the complete formation of the energetically favored, interdigitated gel phase. The noninterdigitated lipids experience enhanced lateral tension, due to the expansion of the growing interdigitated phase within the constant area. The corresponding rise in equilibrium transition temperatures produces supercooled lipids that vitrify when cooled further. Ultimately, this frustrated phase change reflects a coupling between dynamics and thermodynamics and gives rise to an unusual phase coexistence characterized by the presence of two qualitatively different gel phases.

Introduction

The main phase transition of lipid bilayers involves a structural transformation between a high-temperature fluid (liquid-crystalline) and a low-temperature solid or gel.^{1–4} In the fluid phase, the acyl chains are disordered, whereas the gel state is characterized by rigid chains in a crystalline-like lattice. A strongly first-order exothermic process at the phase transition converts the fluid phase into the gel state by facilitating (1) an abrupt rise in chain conformational order, (2) a large contraction in molecular area, and (3) a precipitous drop in the translational mobility of constituent lipids. Precise properties of this main phase transition depend on the molecular characteristics of the lipid, e.g., the acyl chain length, the degree of saturation, and the type of polar headgroup.

In 1998, Hirsh and co-workers reported an unusual structural change during the main phase transformation of aqueous phase aggregates (e.g., multilamellar vesicles) of monofluorinated phospholipid (e.g., 1-palmitoyl-2-(16-fluoropalmitoyl)-*sn*-glycero-3-phosphocholine, F-DPPC, C₄₀H₇₉FNO₈P). This synthetic lipid, obtained by substituting a single fluorine atom on the methyl terminus of the *sn*-2 chain of its natural analogue, 1-palmitoyl-2-(palmitoyl)-*sn*-glycero-3-phosphocholine (DPPC), exhibits surprisingly different thermal properties. Its main phase transition (1) is noticeably more energetic (9.78 kcal/mol compared to 8.7 kcal/mol for DPPC⁵), (2) occurs at about 50 °C, ~10 °C higher than the *T_m* for DPPC, (3) exhibits a rather broad transition width of ~3 °C, and (4) does not reveal the characteristic pretransition (35 °C for DPPC) associated with the formation of the so-called “ripple” phase.

Most remarkably in its fluid phase F-DPPC adopts a typical bilayer motif, but in the gel phase it converts into a fully interdigitated “monolayer” motif.⁵ Stabilization of an interdigitated motif in the gel state can be explained in terms of the balance of competing interactions. The terminal C–F bond is

highly polarized. The affinity of this strong dipole for the polar aqueous environment (and the PC headgroup region) favors full interdigitation. This tendency competes with the likelihood of exposing the hydrophobic methyl terminus on the *sn*-1 chain (as well as nearby methylenes) to the polar surroundings. In the fluid phase, the hydrophobic penalty can be expected to dominate, thus embedding the polar C–F bond within the hydrophobic core of the noninterdigitated bilayer. In the gel phase, however, high conformational order and the attendant tighter packing of the acyl chains reduce the risk of exposing the hydrophobic moiety to the polar region, thus allowing for stabilization of the interdigitated monolayer motif.

The unique structural reorganization during the main phase change in F-DPPC has important consequences for the spatial (re)organization of the bilayer during a phase change. For typical (nonfluorinated) lipids, the fluid–gel transition results in reduced in-plane areas due to increased chain ordering and more efficient packing of acyl tails. Indeed, ~10–20% reduction in surface area following the fluid–gel transition has been typically observed for phosphocholine lipids.^{8,9} In sharp contrast, for F-DPPC bilayers this ordering-induced areal contraction during the fluid-to-gel transition is offset by a dramatic ~50% increase in the in-plane area due to the change in packing motif from the bilayer to the interdigitated monolayer configuration. Together, these processes result in a net anomalous areal expansion (and thickness reduction) that accompanies the main liquid to solid phase transition in F-DPPC.

In closed vesicles, even radical morphological changes following the fluid–gel phase transition such as in F-DPPC bilayers are readily accommodated by corresponding changes in vesicle dimensions.^{10,11} However, how do constrained bilayer configurations (e.g., planar supported lipid bilayers) resolve such large-scale structural changes? Here, we demonstrate that the fluid–gel phase transformation of isolated macroscopic patches of single F-DPPC bilayers confined to the aqueous interface of planar solids progresses under an essentially constant area constraint. Specifically, we find that the macroscopic area of the bilayer patches does not increase despite the availability of

* Corresponding author. E-mail: anparikh@ucdavis.edu.

[†] Lawrence Berkeley National Lab.

[‡] Biophysics Graduate Group, University of California.

[§] Department of Applied Science, University of California.

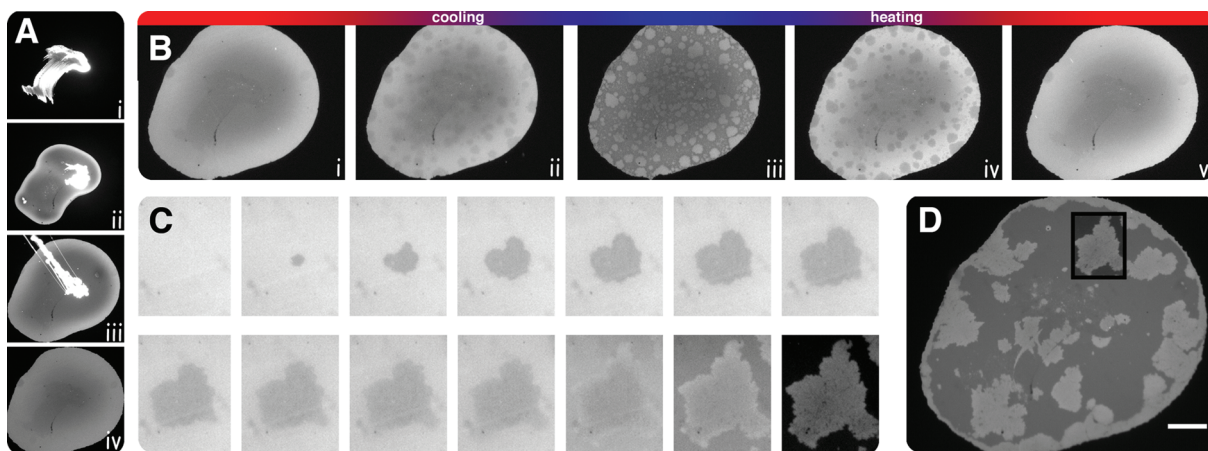


Figure 1. (A) Selected images from a time-lapse epifluorescence movie (0, 23, 440, and 478 s) depicting the surface spreading of a single bilayer following the hydration of the source F-DPPC lipids onto a coverslip glass at $>53\text{ }^{\circ}\text{C}$. (B) Frames from an epifluorescence movie at selected temperatures (55.6, 51.5, 21.3, 52.5, and $57.9\text{ }^{\circ}\text{C}$) during a cooling/heating thermal cycle of an F-DPPC supported bilayer patch cooled at the rate of $8.4\text{ }^{\circ}\text{C}/\text{min}$. (C) A time-lapse series (15 s between frames) of epifluorescence images depicting the formation and fluorescence inversion of the domain highlighted in Figure 1D. (D) Epifluorescence image of the F-DPPC bilayer patch cooled to room temperature at the slower rate of $0.5\text{ }^{\circ}\text{C}/\text{min}$. (Scale bar: $100\text{ }\mu\text{m}$.)

lipid-free surrounding areas. The observation of early gel-phase domains near the free edges of the bilayer patches suggests the role of hindered lateral spreading in imposing the constant area constraint. A qualitatively significant consequence of this constraint is to limit the formation of the thermodynamically favored interdigitated phase during its main phase transition. This in turn produces a novel microstructure consisting of gel-phase domains of interdigitated lipids in a stable coexistence with a quenched,¹² noninterdigitated bilayer in the surrounding phase.

The work reported here offers an initial insight into how small variations in membrane molecular properties can tilt the balance of interactions that control membrane organization, producing large-scale morphological reorganizations. While fluorinated analogues used in the present study are not found naturally in living systems, they nonetheless enable systematic fundamental studies of intermolecular interactions in controlling macroscopic membrane organization. We envisage that such molecules⁶ may offer interesting biocompatible lipid candidates in designing hybrid material systems⁷ with designed biological functionality such as needed for synthetic biology.

Results

The thermotropic phase behavior of F-DPPC bilayers is elucidated using temperature-dependent epifluorescence measurements. We begin with the preparation of isolated patches of single, supported F-DPPC bilayers by adapting the lipid spreading technique.^{13,14} Briefly, single spots of dried F-DPPC (containing 1 mol % fluorescent probe lipid, 1,2-dihexadecanoyl-sn-glycero-3-phosphoethanolamine, triethylammonium salt, and Texas-red labeled DHPE) are transferred onto a clean coverglass by gentle stamping. That the incorporation of the probe lipid, namely, Texas-Red DHPE, does not perturb the thermotropic behavior of F-DPPC was confirmed by comparing thermograms obtained in differential scanning calorimetry (DSC) measurements for pure F-DPPC and dye-doped F-DPPC samples. These results confirm that the presence of the dye neither displaces (to within $0.5\text{ }^{\circ}\text{C}$) nor broadens the main F-DPPC phase transition (see Supporting Information for details). Subsequently, the lipid drop is hydrated by pure water and heated to $60\text{ }^{\circ}\text{C}$, well above the T_m ($50\text{ }^{\circ}\text{C}$) for F-DPPC. The sequence of epifluorescence images shown in Figure 1A(i–iv) confirms the

gradual surface dispersal and lipid spreading. Within $\sim 5\text{--}7\text{ min}$, the surface spreading is completed, producing a macroscopic patch of uniform fluorescence with rounded edges. Fluorescence recovery after photobleaching (FRAP) measurements indicates that the patch is fluid at $53\text{ }^{\circ}\text{C}$, and companion ellipsometric characterization¹⁵ establishes that the final morphology of the spread lipids consists of a single lipid bilayer interfaced to the underlying glass by a thin water film.⁴ The resulting single, supported lipid bilayer patches of F-DPPC are subject to multiple thermal cycles between 58 and $21\text{ }^{\circ}\text{C}$ spanning its T_m (52°). Epifluorescence images in Figure 1B show representative snapshots from an image sequence at selected temperatures during both the cooling and the heating regimes of a typical thermal cycle.

Initially, at $>55\text{ }^{\circ}\text{C}$ the fluorescence emission from the bilayer patch is largely uniform. At $\sim 52\text{ }^{\circ}\text{C}$, this homogeneous fluorescence is abruptly replaced by an inhomogeneous one composed of discrete, irregularly shaped microscopic spots of diminished fluorescence. Because Texas red-DHPE partitions preferentially into the fluid phase,¹⁶ its exclusion from the spots suggests that they represent domains of a growing gel phase. Indeed, a simple fluorescence recovery after photobleaching (FRAP) measurement performed over single probe-depleted domains confirms that at about $52\text{ }^{\circ}\text{C}$ the domains are not fluid, while the surrounding areas are (see below). This observation is in excellent agreement with previous X-ray diffraction and NMR measurements of F-DPPC multilamellar vesicle suspensions, which establish that the fluid–gel phase transition in F-DPPC bilayers occurs at $\sim 50\text{ }^{\circ}\text{C}$.⁵

The transformation of the fluid bilayer to the gel phase does not complete at $52\text{ }^{\circ}\text{C}$ even upon extended standing at this temperature. The sequence of fluorescence images in Figure 1C illustrates that the domains continue to grow until the temperature of $\sim 48\text{ }^{\circ}\text{C}$ is reached. The existence of such a large width of transition ($\sim 4\text{ }^{\circ}\text{C}$) and attendant coexisting gel–fluid phases noted above reflects the low cooperativity of the fluid–gel main phase transition. Such low cooperativity or continuous first-order transitions are pervasive among phospholipid phases.¹⁸ They are consistent with low line tension between the fluid and gel state and arise due to a combination of factors including (1) the softening of the interface due to appearance of conformationally distinct states near the domain interfaces, (2) elastic

strains at the fluid–gel interphase region, (3) electrostatic interactions, and (4) kinetic effects due to limited ensemble dimensions. Because the height difference between the coexisting F-DPPC fluid bilayer and interdigitated gel monolayer states is likely to be significant, the observed width of transition probably suggests the roles of elastic stresses and changes in the dipole interactions during the phase change.

At about 48 °C, a striking inversion of fluorescence contrast occurs: the initial fluorescence pattern of dark domains in brighter surroundings is abruptly replaced by brighter domains in a darker background. During subsequent cooling to room temperature, this new fluorescence contrast persists, and the domain morphology remains unperturbed. This contrast inversion signals a significant structural change such as established in independent lines of experiments (see below).

Upon reheating the sample, the microstructure evolution fully reverses. At ~48 °C, the fluorescence contrast inverts again rendering the domains dark and the surrounding bright. Above this temperature, domains continue to shrink and eventually disappear at ~52 °C producing uniform fluorescence across the lipid patch. This behavior is fully reversible in multiple thermal cycles for single F-DPPC bilayer patches.

Epifluorescence images in Figures 1Biii and 1D compare the structural evolution for F-DPPC bilayers cooled to 21 °C at two different cooling rates, namely, 8.4 and 0.5 °C/min, respectively. These images suggest that samples prepared at slower cooling rates produce less numerous but considerably larger domains. These observations agree well with recent studies that show that sparse nucleation of the gel-phase clusters at slower cooling rate accounts for larger domain formation.¹⁹ Furthermore, despite large variations in cooling rates, the fractional bilayer in the domain phase (0.4–0.5), or the gel/fluid ratio, remains largely invariant.

It is notable that during the entire course of the cooling (or heating) the macroscopic size and shape of the lipid patch (Figure 1B and Supporting Information, video) remains macroscopically constant. This is particularly intriguing since the bilayer area changes during the phase change are expected to be substantial (see above). Furthermore, the edges of the bilayer patch reveal a substantially higher concentration of gel-phase domains at all temperatures in the phase coexistence regime. This effect is even more pronounced in slow-cooled samples (Figure 1C). We reason that an early gelation near the free edges of the bilayer patch hinders the lateral spreading of the bilayer, thus producing a constant area constraint despite the availability of lipid-free areas surrounding the patch. Note also that the ellipsometry and atomic force microscope (AFM) images suggest that the bilayer topography remains planar, adherent to the underlying glass, likely due to strong membrane–substrate interactions. Together these observations establish that the fluid–gel phase transformation in supported F-DPPC bilayers occurs under constant area and topography constraints.

Additional experiments were performed to characterize the structural attributes of the F-DPPC bilayer below 48 °C.

First, we performed a temperature-dependent FRAP experiment. In this adaption of microscopy-based FRAP, the thermal onset of long-range translational mobilities for lipids in domains and the surrounding background phase are probed. As seen in Figure 2ii, single microscopic spots are first photobleached within the domain and the surrounding phase at room temperature (21 °C) using a focused excitation laser. At this temperature, neither spot exhibits any blurring or recovery upon standing suggesting that lipids in both the domains and the surrounding phase are immobile. Subsequently, the sample

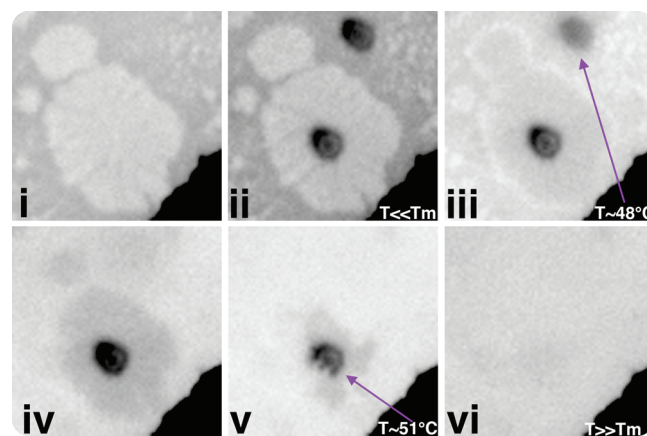


Figure 2. Spots are laser-bleached into both the domain and the surrounding areas at room temperature, and then the sample is heated until both spots blur and recover in intensity. Bar scales to 50 μm.

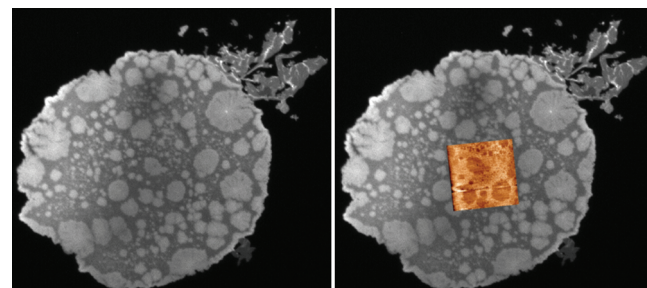


Figure 3. Left: A room-temperature fluorescence image of an F-DPPC membrane patch on glass. Right: The same image but overlaid with a contact-mode AFM scan showing that the domains are of diminished height. AFM region scales to 90 μm a side.

temperature is gradually increased, and the spot properties are monitored (FRAP²⁰). Fluorescence images shown in Figure 2iii and 2v reveal that the photobleached spot in the surrounding phase begins to blur at 48 °C, whereas that in the domain phase reveals blurring (and subsequent recovery) only after 51 °C is crossed. The latter is entirely consistent with observations of the appearance of gel-phase domains at the same temperature during the cooling phase of the thermal cycle and with previous studies of thermodynamic main phase transition temperature in F-DPPC suspensions. The former, on the other hand, indicates a marked change in the surrounding background at ~48 °C from a gel-like state characterized by the loss of long-range fluidity to a high-temperature fluid phase. This change in the F-DPPC surrounding phase coincides well with the abrupt fluorescence contrast inversion observed at 48 °C. The latter can arise either due to physical exclusion of the probe lipids or due to the substantial changes in their molecular environment. The precise origin of the contrast inversion notwithstanding, these two coincident changes signal a gel-like phase formation in the surrounding phase below this temperature.

Second, to compare physical thicknesses of the two coexisting gel-like phases, we performed atomic force microscopy (AFM) measurements. These data for F-DPPC samples at room temperature (Supporting Information, *image*) reveal that the domains are topographically lower than the surrounding background (see Figure 3). A closer comparison of the height disparity between the domain and the background from several different ($N = 47$) locations within a single sample yields a mean value of 1.4 ± 0.3 nm. Assigning the domain-associated gel phase to the interdigitated F-DPPC monolayer, the taller surrounding phase is most likely a noninterdigitated bilayer.

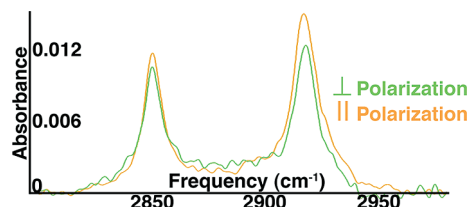


Figure 4. Room-temperature polarized FTIR spectra of an F-DPPC bilayer formed on a silicon ATR crystal. Prior to acquiring the spectrum, the bilayer was temperature cycled through the melting temperature to form domains whose presence was confirmed with fluorescence microscopy.

Although direct comparison with previous studies is unavailable, a comparison between the thicknesses of unsupported gel-phase DPPC and F-DPPC, which are of comparable molecular lengths, is instructive. In the gel phase, the difference in the X-ray repeat period for noninterdigitated DPPC bilayers (6.3 nm) and interdigitated F-DPPC monolayers (5.0 nm) is 1.3 nm, remarkably similar to that derived in our AFM measurements.⁵

Third, to examine if the two coexisting gel-like phases differ in their chain molecular structure, we carried out attenuated total reflection Fourier-transform infrared (ATR-FTIR) spectroscopy measurements. Spectral traces for the s- and p-polarized attenuated total reflection of F-DPPC bilayers at room temperature in the 2800–3000 cm⁻¹ region are shown in Figure 4. Both s- and p-polarized traces reveal two discernible peaks with their peak maxima at 2850 and 2917 cm⁻¹. These peaks can be straightforwardly assigned to methylene symmetric, d^+ , and antisymmetric, d^- , stretching mode absorptions. The exact locations of these peaks are well-known diagnostic markers of acyl chain-conformational order. In solid crystalline phases, the symmetric methylene stretching (d^+) of alkyl chains absorbs between 2848 and 2850 cm⁻¹, and the asymmetric stretching (d^-) occurs between 2916 and 2918 cm⁻¹. For a conformationally disordered liquid phase, however, absorptions due to d^+ and d^- modes occur at distinctly higher ranges of 2852–2854 and 2924–2928 cm⁻¹, respectively. Although, contributions from the domain and the surrounding phases cannot be isolated, the observed average values for methylene stretching peaks indicate that both coexisting phases are characterized by conformationally ordered chains. Thus, the two coexisting thermodynamic and nonthermodynamic phases can be differentiated neither in terms of their lateral fluidity nor in terms of their chain conformational order but require a second-order parameter based on the presence or absence of interlayer interdigitation.

Discussion

The evidence presented in this study establishes that the fluid to gel phase transformation in isolated patches of supported F-DPPC bilayers remains incomplete. It occurs under an extraneously imposed constant area and constant planar topology constraints. Upon passage through the transition temperature, the high-temperature homogeneous F-DPPC phase transforms into a microphase-separated state characterized by a stable coexistence of distinct gel-like phases. The domain-associated gel phase represents the thermodynamically favored, interdigitated F-DPPC monolayer consisting of ordered assemblies of acyl tails. The precise nature of the ordering may be accessible by recent molecular-scale AFM imaging techniques.¹⁷ The immobile gel-like phase in the surrounding background also consists of conformationally ordered acyl tails but remains a noninterdigitated bilayer in a frozen or glassy-like state.

All of the results presented here can be reconciled in terms of a generic mechanistic pathway in which externally imposed area and topography constraints frustrate the main phase transition between the high-temperature fluid and the low-temperature gel phases.

In free vesicular aggregates, the main phase transition occurs under variable area conditions that can restore constant surface tension. In the confined bilayer configuration studied here, the anomalous area expansion during the extended and continuous fluid to gel transition requires that the phase change proceeds under conditions of variable surface tension. As the incipient gel-phase domains grow within the phase transition window, lateral tension in the compressed residual fluid must necessarily increase. This continuous shift in surface tension must result in a corresponding shift in the equilibrium transition temperature. Because the gel to fluid ratio does not appear to be rate dependent in our measurements, it seems reasonable to assume that gel to fluid ratios are at equilibrium during the transition. In the thermodynamic limit, a relationship between these two quantities can be found, in terms of transition temperature of free bilayers, using the two-dimensional version of the Clausius–Clapeyron equation^{18,21}

$$\frac{dT_m}{d\Pi} = T_m \frac{\Delta A_o}{\Delta H_o} \quad (1)$$

where T_m is the phase transition temperature; Π is the surface tension; ΔA_o is the change in molecular area; and ΔH_o is the melting enthalpy. The change in melting temperature is then straightforwardly related to the fraction of the patch area that interdigitates (q) and the net increase in molecular area of the interdigitated lipids (c) by eq 2 (see Supporting Information for full derivation of the approximation, *text*).

$$\Delta T_m = \frac{\ln\left(\frac{1-q}{1-\frac{q}{c}}\right)}{K - \kappa\beta} \quad (2)$$

Using typical lipid bilayer values¹⁸ of the thermal expansion coefficient (K , 5×10^{-3} K⁻¹), compressibility (κ , 6.9 m² J⁻¹), and beta ($\beta = (\Delta H_o)/(T_m \Delta A_o)$, 2.16×10^{-3} J m⁻² K⁻¹), a rough estimate of the tension-dependent transition temperature can be made. The net increase in the molecular area of the interdigitated lipids, c , is approximated by a gelling-induced contraction of 20% and an interdigitation-induced doubling in molecular area. Following the analysis above we estimate the increase in the phase transition temperature to climb gradually and monotonically as q increases. Eventually the growth of the interdigitated region is arrested, probably limited by the increased pressure exerted by the residual fluid phase. The fraction of the area that ultimately interdigitates ($q = 0.4$, in Figure 1D) indicates that the phase transition temperature of the residual lipids exhibits a continuous and gradual increase by as much as 22 °C. As the interdigitated phase grows, the equilibrium phase transition temperature of the residual lipids climbs beyond the current temperature, yet they remain fluid in supercooled metastable states.

On the basis of the considerations above, we propose that the unusual microstructure evolution during the main phase transition of F-DPPC results from the novel variable surface tension conditions which arise during the course of the phase transition (see Figure 5). In particular, the formation and growth of the incipient gel-phase domains of increased molecular area raises the surface tension of the surrounding fluid lipids during the phase change under constant area (and topology) constraints.

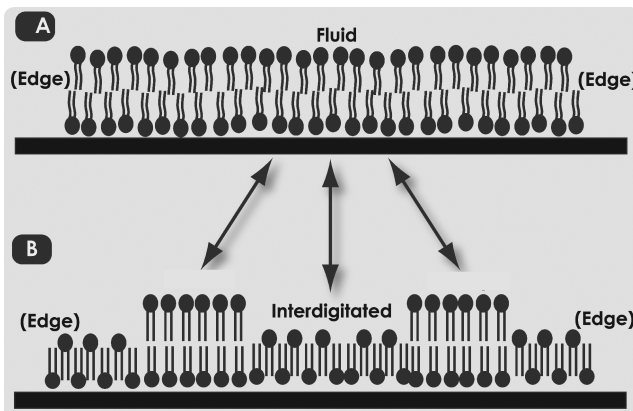


Figure 5. Sketch of the frustrated phase transition's proposed microstructure evolution.

(Were the constant area constraints absent, we would expect the lipid patches to expand laterally in a manner consistent with reports of ethanol-induced interdigitation of fluid bilayers.²²) This in turn dynamically raises the fluid–gel transition temperature for the residual lipids above the experimental temperature, producing a supercooled lipid state. Further cooling quenches the disordered fluid phase as a noninterdigitated, immobile bilayer; the dynamic readjustment of the phase transition conditions frustrates its thermodynamic conversion into the interdigitated state. The net result of this frustration is to produce a novel phase coexistence in F-DPPC supported bilayers consisting of equilibrium gel phase domains of interdigitated lipids surrounded by an immobilized bilayer in a glassy-like or jammed state.

These results exemplify the broadly relevant issue of microstructure evolution during phase changes in complex fluids. They illustrate coupling between dynamics and thermodynamics in condensed phase systems. In this case, the constant area constraint imposed by the early gelation at the boundaries of the laterally contiguous fluid bilayer patch couples with limited phase transition cooperativity common among lipid mesophases to dynamically modulate the phase transition conditions. These conditions allow for the formation of metastable supercooled states which decrease the nucleation rate and increase the free energy barrier for the formation of the new phase.²³ The final incomplete gelation that produces the coexisting gel states reveals how the growing lateral stress imposed by the incipient phase change directly influences the course, kinetics, and equilibration of the residual fluid.

Materials and Methods

To simultaneously observe the bulk and edges of a supported membrane, we create localized patches of lipid bilayers by adapting a well-known lipid spreading technique.^{13,4,14} Approximately 1 μL of a lipid/dye/chloroform mixture is deposited on the tip of a downward pointing sharp metal or glass pin and dried under vacuum in the dark for at least 2 h. The mixture is a 7 mg/mL solution of F-DPPC doped with 1 mol % Texas Red DHPE (purchased from Invitrogen) fluorescent dye. Pressing the sharp, lipid-caked tip against a clean plasma-etched glass coverslip for 1–2 s transfers lipid material to the substrate (creating the “source”). When the source is hydrated and heated above its phase transition temperature ($\sim 53^\circ\text{C}$), lipids spread outward until the source is depleted, creating a continuous and uniform single bilayer patch (see Figure 1A). Applying a current

of water over the patch with a pipet rinses away excess lipid material at the source and arrests spreading. This leaves a discrete surface film patch consisting of a single lipid bilayer, as confirmed by FRAP-measured fluidity above 53°C (see Figure 2), AFM (see Figure 3), and ellipsometry¹⁵ (on the surface oxide of polished Silicon, not shown here). The patches were observed with a fluorescence microscope (TE2000, Nikon) coupled to an automated translation stage and temperature control, and relative height data were determined with a Veeco Dimension 3100 AFM. ATR-FTIR spectra were recorded using a Bruker Equinox 55 Fourier transform infrared spectrophotometer equipped with a horizontal ATR accessory (Spectra-Tech, Inc., Shelton, CT) and DTGS detector (Bruker, Göttingen, Germany).

Acknowledgment. This work was carried out under a grant from U.S. Department of Energy's Biomolecular Materials Program (DE-FG02-04ER46173). B.S. and A.W.S. are supported by fellowships from University of California's Graduate Research and Training Program in Adaptive Biotechnology (GREAT) and the UEPP Fellowship from the Physical Bioscience Institute at LLNL, respectively. We thank R. El-Khoury, M. Vinchurkar, M. Salmeron, P.D. Ashby, and A.M. Smith for their help and A. Janshoff for insightful comments.

Supporting Information Available: A video of heating/cooling cycles of a typical F-DPPC membrane patch; DSC results and analysis of the influence of 1% Texas Red conjugated lipid on F-DPPC phase behavior; and analytical derivation of the pressure induced change in bilayer phase transition temperature. This material is available free of charge via the Internet at <http://pubs.acs.org>.

References and Notes

- (1) Nagle, J. F. *Ann. Rev. Phys. Chem.* **1980**, *31*, 157–196.
- (2) Sackmann, H.; Demus, D. *Mol. Cryst. Liq. Cryst.* **1966**, *2*, 81–102.
- (3) Mouritsen, O. G.; Jorgensen, K. *Chem. Phys. Lipids.* **1994**, *73* (1–2), 3–25.
- (4) Sackmann, E. *Science* **1996**, *271*, 5245.
- (5) Hirsh, D. J.; Lazar, N.; Wright, L. R.; Boggs, J. M.; McIntosh, T. J.; Schaefer, J.; Blazyk, J. *Biophys. J.* **1998**, *75*, 1858–1868.
- (6) Schuy, S.; Faiss, S.; Yoder, N. C.; Kalsani, V.; Krishna, K.; Janshoff, A.; Vogel, R. *J. Phys. Chem. B* **2008**, *112*, 8250–8256.
- (7) Riess, J. G. *Curr. Opin. Colloid Interface Sci.* **2009**, *14*, 294–304.
- (8) Evans, E.; Needham, D. *J. Phys. Chem.* **1987**, *91*, 4219–4228.
- (9) Feng Xie, A.; Yamada, R.; Gewirth, A. A.; Granick, S. *Phys. Rev. Lett.* **2002**, *89*, 2461031II2461034.
- (10) Solon, J.; Pécreaux, J.; Girard, P.; Fauré, M. C.; Prost, J.; Bassereau, P. *Phys. Rev. Lett.* **2006**, *97*, 98103.
- (11) Heimburg, T. *Biochim. Biophys. Acta* **1998**, *1415*, 147–162.
- (12) Debenedetti, P. G.; Stillinger, F. H. *Nature* **2001**, *410*:6825, 259–267.
- (13) Nissen, J.; Gritsch, S.; Wiegand, G.; Rädler, J. O. *Eur. Phys. J. B-Condens. Matter* **1999**, *10*, 335–344.
- (14) Sanii, B.; Parikh, A. N. *Soft Matter* **2007**, *3*, 974–977.
- (15) Howland, M. C.; Szmodis, A. W.; Sanii, B.; Parikh, A. N. *Biophys. J.* **2007**, *92*, 1306.
- (16) Baumgart, T.; Hunt, G.; Farkas, E. R.; Webb, W. W.; Feigenson, G. W. *Biochim. Biophys. Acta* **2007**, *1768*, 2182–2194.
- (17) Asakawa, H.; Fukuma, T. *Nanotechnology* **2009**, *20*, 264008.
- (18) Charrier, A.; Thibaudau, F. *Biophys. J.* **2005**, *89*, 1094–1101.
- (19) Blanchette, C. D.; Lin, W. C.; Ratto, T. V.; Longo, M. L. *Biophys. J.* **2006**, *90*, 4466–4478.
- (20) Axelrod, D.; Koppel, D. E.; Schlessinger, J.; Elson, E.; Webb, W. W. *Biophys. J.* **1976**, *16*, 1055–1069.
- (21) Wolfe, J.; Bryant, G. *Cryobiology* **1999**, *39*:2, 103–129.
- (22) Gedig, M.; Faib, S.; Janshoff, A. *Biointerfaces* **2008**, *3* (2), FA51.
- (23) Evans, R. M. L.; Poon, W. C. K.; Cates, M. E. *Europhys. Lett.* **1997**, *38* (8), 595–600.